

RSC Advances



This is an *Accepted Manuscript*, which has been through the Royal Society of Chemistry peer review process and has been accepted for publication.

Accepted Manuscripts are published online shortly after acceptance, before technical editing, formatting and proof reading. Using this free service, authors can make their results available to the community, in citable form, before we publish the edited article. This *Accepted Manuscript* will be replaced by the edited, formatted and paginated article as soon as this is available.

You can find more information about *Accepted Manuscripts* in the [Information for Authors](#).

Please note that technical editing may introduce minor changes to the text and/or graphics, which may alter content. The journal's standard [Terms & Conditions](#) and the [Ethical guidelines](#) still apply. In no event shall the Royal Society of Chemistry be held responsible for any errors or omissions in this *Accepted Manuscript* or any consequences arising from the use of any information it contains.

Fabrication of thick-walled polyacrylonitrile (PAN) with high uniformity by an easily assembled double-T droplet generator

Hao Peng^{a,b}, Meifang Liu^b, Jing Li^b, Sufen Chen^b, Zhanwen Zhang^b, Bo Li^{b,*}, Liqin Ge^{a,*}

Abstract

Low density carbon shells were required in the inertial confinement fusion (ICF) experiments. Polyacrylonitrile (PAN), as a common raw material of carbon, was studied and adopted to prepare thick-walled microspheres with the outer diameter ranging from 300 μm to 800 μm ; wall thickness around 50 μm – 120 μm ; sphericity (OOR): <2 μm ; and wall thickness uniformity (ΔT_w): <9 μm . The preparation of PAN microspheres were based on an assembled double T-junction droplet generator. The major challenge in this experiment was to simultaneously meet the requirements and restrictions on both wall thickness and its uniformity. In order to improve the wall

^aState Key Laboratory of Bioelectronics, School of Biological Science and Medical Engineering, Southeast University, Nanjing 210096, P. R. China

^bLaser Fusion Research Center, China Academy of Engineering Physics, Mianyang 621900, P. R. China

Tel.: +86 025 83619983; fax: +86 025 83795635.

E-mail address: lqge@seu.edu.cn, lb6711@126.com.

uniformity of thick-walled PAN microspheres, two major factors, the viscosity and the temperature which affect the density-matching solutions between the O_1/W compound droplet and the O_2 phase, were tested. The calculated results of OOR and ΔT_w showed that the optimal density gap between the O_1/W compound droplet and the O_2 phase would be around 0.015 g/cm^3 when the temperature is at $10 \text{ }^\circ\text{C}$ or the viscosity ratio λ is near 3.6 times (the viscosity ratio λ is defined as the ratio of the W phase to the O_2 phase). Under this circumstance, the wall thickness uniformity and sphericity were largely improved. Furthermore, the experiment established that wall thickness uniformity was more sensitive to the temperature and the viscosity than the sphericity.

Keywords: PAN microspheres, density matching, sphericity, wall thickness uniformity, droplet generators, ICF targets

1. Introduction

Carbon, as a new inorganic material, has the characteristics of high intensity, thermostability, anti-corrosion, radio-resistance, low density, *etc.* These features make it a high-powered material [1]. Recently, carbon materials have been widely applied in aviation, national defense, sports equipment, medical instruments, *etc.* [2]. And low density carbon targets are used to study fusion project. The aim is to produce low density foam shells composed of mostly C and a small amount of other elements in accordance with strict specifications. In the experiment of laser inertial confinement

fusion (ICF), the targets were used as carriers in loading fuel gas of deuterium and tritium for the inertial confinement fusion reaction. The most important factor is the property of the microspheres capsule which directly affects the success of the experiment. However, different ICF target materials presented separate advantages and limitations, wherein the polymeric hollow microspheres focusing on a wide variety of polymeric materials. The criteria of ICF targets are listed as follows: outer diameter should be limited within 300 μm to 800 μm , wall thickness should be about 50 μm – 120 μm , sphericity (OOR) : $<2 \mu\text{m}$, and wall thickness uniformity (ΔT_w) : $<9 \mu\text{m}$ [3,4].

The performances of a carbon complex depend on its precursor, and theoretically, a good precursor should have a high carbon content [5], high molecular weight [6, 7], and a high degree of molecular orientations [7-9]. Polyacrylonitrile (PAN)-based carbon seems to be the optimal choice for this experiment because it can meet all of these requirements [10]. To obtain carbon product, the PAN fibers are heated in air at temperature around 200 $^{\circ}\text{C}$ – 300 $^{\circ}\text{C}$, and then carbonized in an inert atmosphere at a temperature above 1,000 $^{\circ}\text{C}$ [11]. More specifically, the preparation of low density carbon foam shells can be divided into two parts: the first part represents the preparation process of required thick-walled PAN microspheres based on an assembled double T-junction droplet generator, and the second part includes the carbonization of PAN microspheres at high temperature, which further form the

carbon foam shells. In this work, we mainly focused on the preparation of thick-wall PAN microspheres, which will meet the ICF requirements in the future.

During the last few years, the developments of PAN microspheres have allowed for meeting the specific requirements on its diameter and sphericity. However, it is still difficult to reach the wall thickness variation and thickness uniformity. The influence parameters of thickness uniformity include density, kinetics, deformation, interfacial tension, and viscosity [12]. Density is a key factor among these parameters and the density matching principle was used to improve the thickness uniformity and sphericity of microspheres [13-24]. Therefore, the effect of density on the thickness uniformity of thick-walled PAN microspheres is explored, particularly in this paper, as well as the influence of viscosity on the thickness uniformity of thick-walled PAN microspheres.

2. Experimental

2.1 Materials

N, N-dimethylformamide (DMF) was obtained from Sinopharm Chemical Reagent Shanghai Co. Ltd, Polyacrylonitrile (PAN, $M_w = 60,000$) was purchased from Tri-high Membrane Technology Co. Ltd, China. Aliquat 336 was bought from Alfa Aesar, England. The silicone oil was procured from Shinetsu Chemical Co. Ltd. Japan. Deionized water was laboratory homemade. All the materials were used without further purification.

2.2 Preparation of PAN microspheres

2.2.1 Generation of the double emulsion droplets

4.5g PAN powder was dissolved in 30 ml DMF with additional 2 ml Aliquat 336 (it is a kind of surfactant which can reduce the surface tension between the W phase and O phase and it can improve the stability of double emulsion droplets) through stirring with a magnetic stirrer to ensure complete mixing and dissolution of the components to form a 15/100 g·ml⁻¹ PAN solution as the middle phase (W phase), the silicone oil used as both inner phase (O₁ phase) and outer phase (O₂ phase). An easily-assembled double T-junction droplet generator (as shown in Fig. 1a) was fabricated by a Teflon tube and PEEK T-shaped channels (IDEX Health & Science LLC, USA) [25]. Teflon tubes, which are usual liquid chromatography accessories, are resistant to organic solvents due to their oleophobic and hydrophobic properties. The cross-sectional shape of the channels meeting at the T-junction is a 1mm diameter circle that interlinked with the Teflon tube perfectly, and the Teflon tube can be tightly inserted through the PEEK T-shaped channel to prevent liquid leakage. The O₁, W and O₂ phases were pushed into the double T-junction droplet generator by three syringes (10 ml, SGE Analytical Science Pty Ltd.), which were correspondingly propelled by the peristaltic pumps (model LSPP01-1A from Baoding Longer Precision Pump Co. Ltd.), respectively.

All three phases flowed through the Teflon tube, and when the inner phase crossed the middle phase, orderly droplets were generated in the first T-shaped channel. The initial droplets were flowed through the tube which was surrounded by

the middle phase coming across the outer phase at the second T-shaped channel, forming the O_1/W emulsion droplets in the O_2 phase. The O_1/W emulsion droplets were collected in a 1000 ml beaker which is filled with 500 ml O_2 phase. In this work, to limit the possible influence of the microspheres size and wall thickness on the density matching, the inner diameter (I.D.) and wall thickness of the PAN microspheres set as 200 μm and 90 μm , respectively. The size of the microspheres was controlled by changing the flow rates of the O_1 , W, and O_2 phases. The above given diameter and wall thickness ranges were achieved through regulating the flow rates. The experimental results indicate that the I.D. and wall thickness are in the range of $200 \pm 20 \mu\text{m}$ and $90 \pm 10 \mu\text{m}$, respectively.

2.2.2 The solidification of the double emulsion droplets

About 200 pieces of the O_1/W droplets were collected in the beaker. Then the beaker was set into a water bath at the temperature of 5 $^{\circ}\text{C}$, 10 $^{\circ}\text{C}$, 20 $^{\circ}\text{C}$, and 30 $^{\circ}\text{C}$ (Temperature was adjusted by cooling or heating) and stirred vertically at a certain speed (80 rpm) through a blender (EUPROSTAR power control-visc, IKA) until the solvent in the PAN microspheres was evaporated totally (Fig.1b). Repeated experiments showed that the diameters of the PAN microspheres would be fixed during the solidifying process and the color of PAN microspheres would be transparent (the original color of PAN microspheres was faint yellow) which demonstrated the solvent has been totally evaporated. During this solidification

process, the solvent DMF in the O_1/W compound droplets was regarded to be evaporated completely and the hollow PAN microcapsules were obtained.

2.2.3 Fabrication of the solvent-free hollow microcapsules

In 2.2.2 part, we can obtain the hollow PAN microspheres, but the obtained hollow microspheres are full of silicone oil. In order to remove the inner silicon oil, the PAN hollow shells were immersed into silicone oil with different kinetic viscosity distributed from 10 cst, 5 cst, 1 cst to 0.65 cst for 24 hours, respectively. Thus the inner silicone oil (O_1 phase) with high viscosity was replaced step by step. In order to avoid the collapse of the hollow microspheres, supercritical dryer was employed to remove the inner silicon oils of the PAN hollow microspheres (waters supercritical fluid extraction system, SFE 500-2-base, USA) at the temperature of 45 °C for 6h under 280 bar CO_2 pressure and 5g/min flow rate of CO_2 . In this step, we can obtain the solvent-free PAN hollow microspheres.

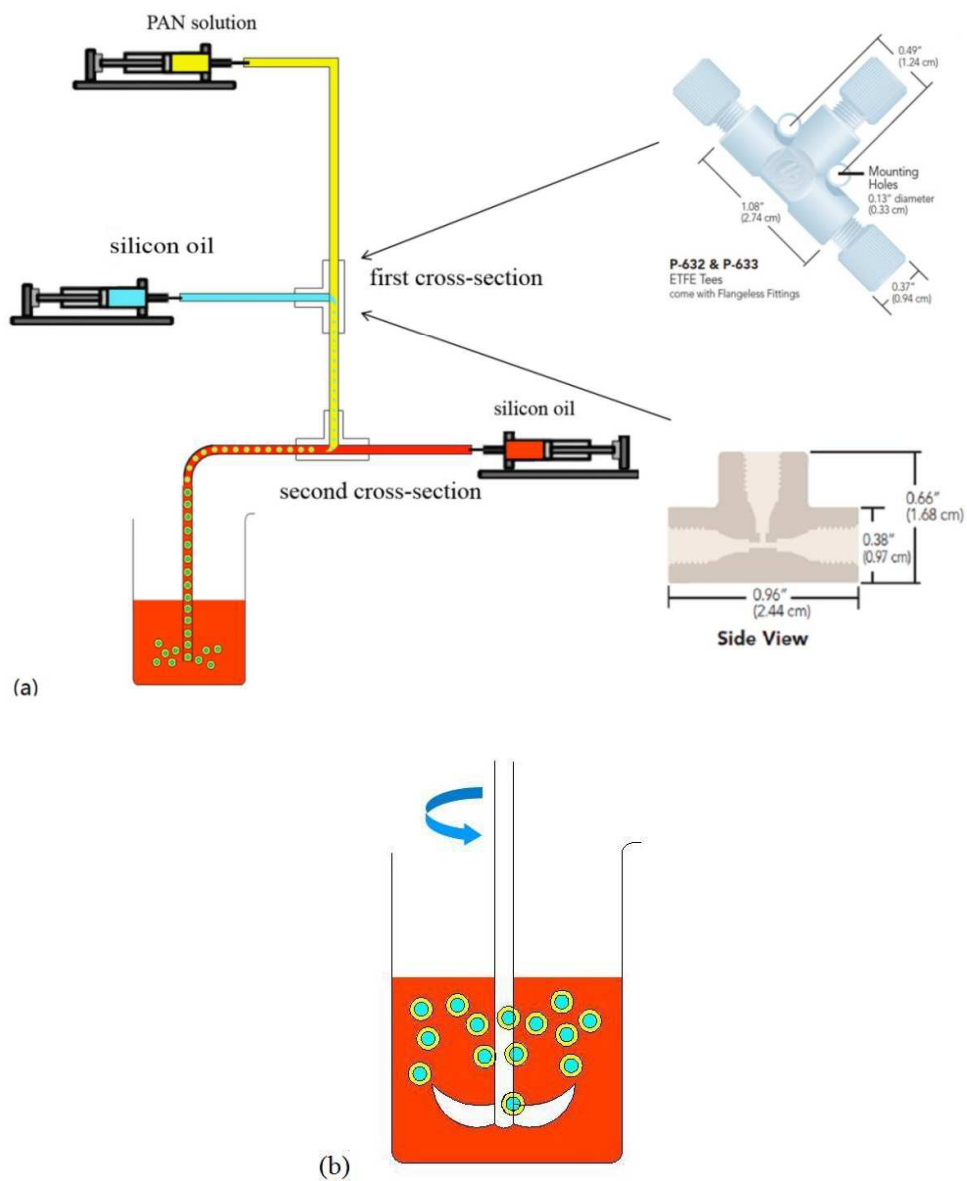


Figure 1. (a) Sketch of the double T-junction droplet generator and droplet formation based on the droplet generator. (b) The solidification of O_1/W compound droplets in O_2 phase stirring with a beaker.

2.3 Characterization

2.3.1 Density and viscosity

The viscosity value of O₁, W, and O₂ phase at different temperature level from 5 °C to 30 °C with a interval of 5 °C were measured precisely by a viscometer (Anton Paar Lovis, 2000M) (Table 1). The density of O₁, W, O₂ phase, and solvent DMF under the same temperature level were measured accurately by a densimeter (Anton Paar[®] DMA 5000). The observed data in this experiment was listed in Table 2. Based on the dimension of the O₁/W compound droplets, the density of W phase (ρ_1), O₁ phase (ρ_{o1}) and solvent DMF (ρ_{DMF}), the average density of O₁/W compound droplets (ρ_i) during the curing process can be calculated using the following equations:

$$\rho_i = \frac{m_{w_i} + m_{o1}}{V_{o1} + V_{w_i}} = \frac{(V_{w_a} \cdot \rho_1 - \Delta V \cdot \rho_{DMF}) + m_{o1}}{V_{w_i} + V_{o1}} \quad (1)$$

$$\Delta V = V_{w_a} - V_{w_i} \quad (2)$$

In the above formulas, m represents the mass and V means the volume.

m_{w_i} is the mass of W phase when the volume fraction of PAN in W phase is P_{w_i} , V_{w_i} is the volume of W phase when the volume fraction of PAN in W phase is P_{w_i} . V_{w_a} is the initial volume of W phase. It is notable that the volume of O₁ phase in the O₁/W compound droplet and the amounts of PAN in the W phase is possible to change within a small range during the solidifying process. In order to eliminate its effects, the deviations in volume of O₁ phase and amounts of PAN were ignored in the process. V_{w_i} , V_{o1} and m_{o1} is calculated with following equations:

$$V_{w_i} = \frac{4}{3} \cdot \pi \cdot (R^3 - r^3) \quad (3)$$

$$P_{w_i} = \frac{V_{w_a} \cdot P_{w_a}}{V_{w_i}} \quad (4)$$

$$V_{ol} = \frac{4}{3} \cdot \pi \cdot r^3 \quad (5)$$

$$m_{ol} = \rho_{ol} \cdot V_{ol} \quad (6)$$

Where the R and r is the outer radius and the inner radius of the O_1/W compound droplet measured by the digital microscope (VHX-600, KEYENCE), respectively (Fig. 2). P_{wa} represents the initial volume fraction of PAN in W phase.

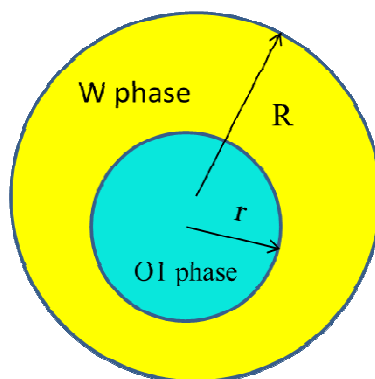


Figure 2. The morphology of O_1/W compound droplet.

Table 1 Viscosity of O_1 , W, and O_2 phase at different temperature.

Temperature/ °C	Viscosity of PAN solution/ (mPa.s)	Viscosity of 50cst silicon oil/ (mPa.s)	Viscosity of 100cst silicon oil/ (mPa.s)	Viscosity of 200cst silicon oil/ (mPa.s)	Viscosity of 350cst silicon oil/ (mPa.s)
5	1724	66.9	142.7	218.6	446.7
10	1442	59.8	126.9	196.6	398.2
15	1237	53.5	113.2	176.9	359.1
20	1067	48.0	101.8	159.9	322.1
25	924.9	43.6	91.7	144.7	292.5
30	792.1	39.5	82.9	131.3	265.2

Table 2 Density of O₁, W, O₂ phase and solvent DMF at different temperature.

Temperature/ (°C)	Density of 15% g/ml PAN solution (W phase)/(g/cm ³)	Density of DMF/ (g/cm ³)	Density of 350cst silicon oil (O ₁ , O ₂ phase) /(g/cm ³)
5	0.988595	0.962914	0.985022
10	0.984207	0.958177	0.980470
15	0.979784	0.953419	0.975935
20	0.975353	0.948653	0.971427
25	0.970914	0.943879	0.966949
30	0.966465	0.939101	0.962492

2.3.2 Sphericity and wall thickness uniformity of PAN microspheres

The morphology of the dried PAN microspheres was characterized by a low energy X-ray camera (XTF5011, Oxford Company, USA). The outer diameter and wall thickness of these microspheres were obtained from six different circumferential directions, respectively. The out-of-round (OOR) was defined as difference between the maximum and the minimum outer radius of microspheres in six directions which was used to characterize the sphericity of PAN microspheres and the wall thickness uniformity (T_w) was interpreted as the maximum and the minimum value of the six measured wall thicknesses of a particular PAN microspheres[22, 24]. The calculation equations were as follow:

$$\text{OOR} = D_{max} - D_{min} \quad (7)$$

$$\Delta T_w = T_{Wmax} - T_{Wmin} \quad (8)$$

Where D_{\max} is the maximum outer diameter and D_{\min} is the minimum outer diameter, $T_{w_{\max}}$ is the maximum wall thickness and $T_{w_{\min}}$ is the minimum wall thickness. The cumulative frequency was defined as the proportion of microspheres with variable ΔTw or OOR in a batch (about 300 microspheres).

3. Results and discussion

3.1. Preparations of thick-walled PAN microspheres

In order to obtain the PAN microspheres with the I.D. of $200 \pm 20 \mu\text{m}$, particularly with a wall thickness of $90 \pm 10 \mu\text{m}$, we conducted an in-depth analysis on the elements that may affect the dimensions of PAN microspheres from mainly two aspects: the volume fraction of the W phase and the flow rates of three additional phases. On one hand, we increased the volume fraction of the PAN solution (W phase) to increase the wall thickness. In the solidification stage, the solvent in the PAN microspheres was totally evaporated, which caused the shrinking of the O_1/W compound droplets' dimensions. Therefore, the less amount of solvent in the O_1/W compound droplets, the larger the wall thickness received from the solidification. In this experiment, we mainly paid attention to the testing of three volume fractions of PAN solution: 10%, 12%, and 15% (the yield of thick-walled PAN microspheres was low when the volume fractions were lower than 10%; the PAN solution possessed of poor fluidity when the volume fractions were higher than 15% which is not conducive to forming double emulsions). The dimension distribution of the PAN microspheres based on the three different volume fractions is shown in the Fig. 3. The data

indicated that the 15% volume fraction of PAN solution is best choice for the formation of thick-walled PAN microspheres in the three volume fractions of PAN solution.

On the other hand, the empirical research has established that the flow rates have a significant impact on the size distribution of microspheres generated by the double T-junction droplet generator. To investigate this influence on forming thick-walled PAN microspheres, we focused on the flow rate ratios between the W phase and the O_1 phase (V_w/V_{o1}), which were feasible with the current experiments' setting. The experiment showed that different V_w/V_{o1} could give rise to the diverse drop sizes. Furthermore, from the iteration of the experiment under different flow rate ratios, V_w/V_{o1} , we found that when the flow rate ratios of V_w/V_{o1} equals 20, the O_1 phase drop was $300\mu\text{m} \pm 20 \mu\text{m}$ and created a large distance between the drops, which led to the formation of solid droplets under the shear force of O_2 phase; when the V_w/V_{o1} is 30, the O_1 phase drop became smaller ($260 \mu\text{m} \pm 20 \mu\text{m}$) but still out of diameter range and the drop distance barely changed. The solid droplets presents what collected were the W phase droplets rather than O_1/W emulsion droplets. This caused the formation of solid droplets, which negatively affected the productivity of PAN microspheres. When managing the flow rate ratios of V_w/V_{o1} to 40, the O_1 phase drop size was $220 \pm 20 \mu\text{m}$ and the space between the drops narrowed, which fit the diameter restriction and effectively reduced the number of solid droplets. Continually increasing the flow rate ratios of V_w/V_{o1} ($V_w/V_{o1} = 50$), the O_1 phase drop size kept

decreasing ($160 \pm 20 \mu\text{m}$) and closer arranged, which made it easily to obtain a compound droplet with several drops inside under the shear force of O_2 phase (Fig.4), Fig.4 shows the scheme of the droplets and its corresponding experimental pictures. This indicated that the higher the flow rate ratios of V_w/V_{o1} are, the smaller the drop size will be. According to this, in the later experiments, we fixed the flow rate ratios of V_w/V_{o1} at 40 to gain the PAN microspheres with an I.D. of $220 \pm 20 \mu\text{m}$ and wall thickness of $90 \pm 10 \mu\text{m}$.

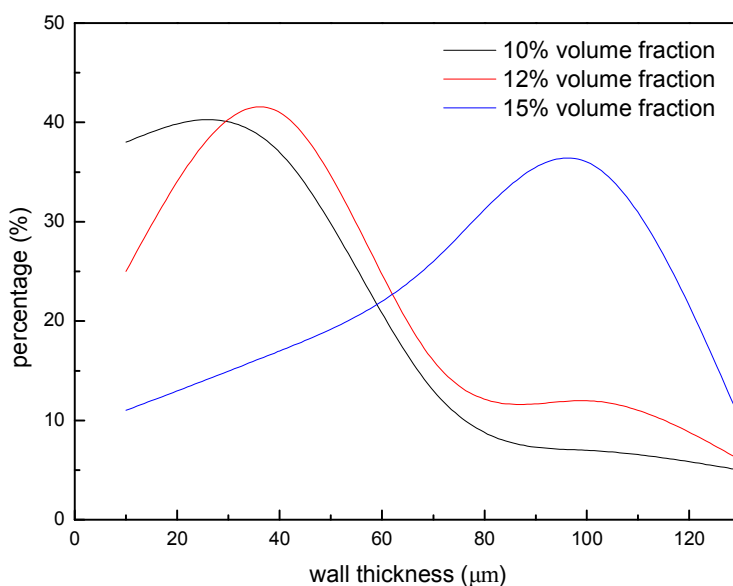


Figure 3. The dimension distribution of the PAN microspheres based on the three different fraction volume fraction of PAN solution.

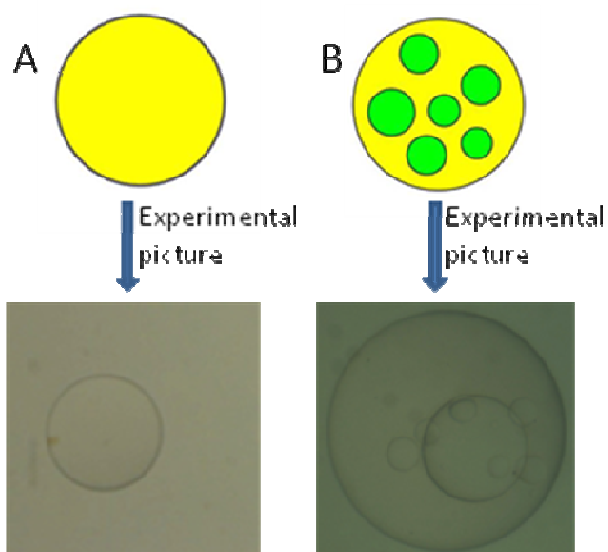


Figure 4. A) Scheme of a solid droplet and its experimental picture. B) Scheme of an emulsion droplet with several drops inside and its experimental picture.

Table 3 The diverse drop size of the O_1 phase in the O_1/W compound droplet at different flow rate ratios V_w/V_{o1} .

flow rate ratios of V_w/V_{o1}	20	30	40	50
the O_1 phase drop size/ μm	300 ± 20	260 ± 20	220 ± 20	160 ± 20

3.2. The temperature effects on the density matching between the O_1/W compound droplet and the O_2 phase

To investigate the role of density matching, the force on a spherical drop of radius R and effective density falling under gravity in a fluid of density were analyzed [27]. In this work, the same mechanics analysis method can be used on the solidifying

temperature effects on the density matching between the O₁/W compound droplet and the O₂ phase. The following three forces act upon the O₁/W compound droplet in the O₂ phase: the weight G (gravity force) of the O₁/W compound droplet, acting vertically downwards through the center of gravity; the upthrust buoyancy (B); and the upwards viscous drag (F) [27].

$$G = \frac{4}{3} \cdot \pi \cdot \rho_{o_2} \cdot g \cdot (R^3 - r^3) \quad (9)$$

$$B = \frac{4}{3} \cdot \pi \cdot \rho_i \cdot g \cdot (R^3 - r^3) \quad (10)$$

$$F = 6\pi \cdot \eta \cdot a \cdot v \quad (11)$$

Here, the ρ_{o_2} is the density of O₂ phase, respectively. And

$$\text{Net downward force} = G - (B + F) \quad (12)$$

This force is responsible for the downward acceleration of the O₁/W compound droplet. A stage is reached when the weight of the spherical drop is just balanced with the sum of the upthrust and viscous drag. At this stage there are no other forces on the O₁/W compound droplet, droplet started to move with terminal velocity v_0 .

$$\frac{4}{3} \cdot \pi \cdot (\rho_i - \rho_{o_2}) \cdot g \cdot (R^3 - r^3) = 6\pi \cdot \eta \cdot a \cdot v \quad (13)$$

$$v = v_0 = \frac{2}{9} \cdot \frac{(\rho_i - \rho_{o_2}) \cdot g}{\eta \cdot a} \cdot (R^3 - r^3) \quad (14)$$

Further, if ρ_i equals to ρ_{o_2} , then v_0 will be 0, and the droplet will maintain in a balance state.

Density matching plays a significant role in the fabrication of microspheres in the emulsion technique. It helps to avoid some asymmetries (elongation or deformation due to gravity) in emulsion droplets and also prevents the sedimentation and creaming of emulsion droplets. Thus, both ultimate sphericity and wall thickness uniformity of microspheres depend on how accurately densities of different phases are matched during the solidifying process [26].

Figure 5 shows the transformation of the O_1/W compound droplet density in accordance with the change of PAN volume fraction at 5 °C, 10 °C, 20 °C, and 30 °C, respectively. The density match index, $\Delta\rho$ (equal to the difference between ρ_i and ρ_{o2}), was defined as the density difference between the O_1/W compound droplet and the O_2 phase at the initial PAN volume fraction (15%). It is proposed to measure the density matching levels between the O_1/W compound droplet and the O_2 phase during the solidifying process [26]. This experiment affirmed that the density difference ($\Delta\rho$) would increase along with the increasing temperature. Additionally, $\Delta\rho$ is almost the same when the degree was at 5 °C and 10 °C (Fig. 5 and Table 4). For the wall thickness uniformity, the ΔTw appeared to have conspicuous disparity when the temperature of solidification was 10 °C, 20 °C, and 30 °C, respectively (Fig. 6a). Nevertheless, the ΔTw exhibited a small distinction between the solidifying temperature of 5 °C and 10 °C. The results correspond with the density gap at different temperatures, and the investigation of OOR indicated that the small OOR value occupied a larger part along with the increasing solidifying temperature (Fig. 6b).

However, the improvement of OOR between 5 °C, 10 °C, and 20 °C shows almost the same tendencies, all of which were better than the OOR at 30 °C. Compared to the wall thickness uniformity and sphericity of ICF targets, the yields of PAN microspheres were around 75% when ΔT_w was less than 9 μm and 84% when OOR was less than 2 μm at the solidifying temperature of 5 °C or 10 °C (Table 4). It can be concluded that the wall thickness uniformity and sphericity appeared to have the most effective enhancement at 10 °C solidifying temperature and the ΔT_w presented a higher sensitivity to the solidifying temperature than the OOR.

The reduced temperature not only shorted the density gap but also delayed the molecule movement. The slow-moving molecule induced the speed of volatilization of solvent DMF. Therefore, the time is enough for the transformation of the droplet, which makes it capable of reaching the objectives of good wall thickness, uniformity, and sphericity (Fig.7).

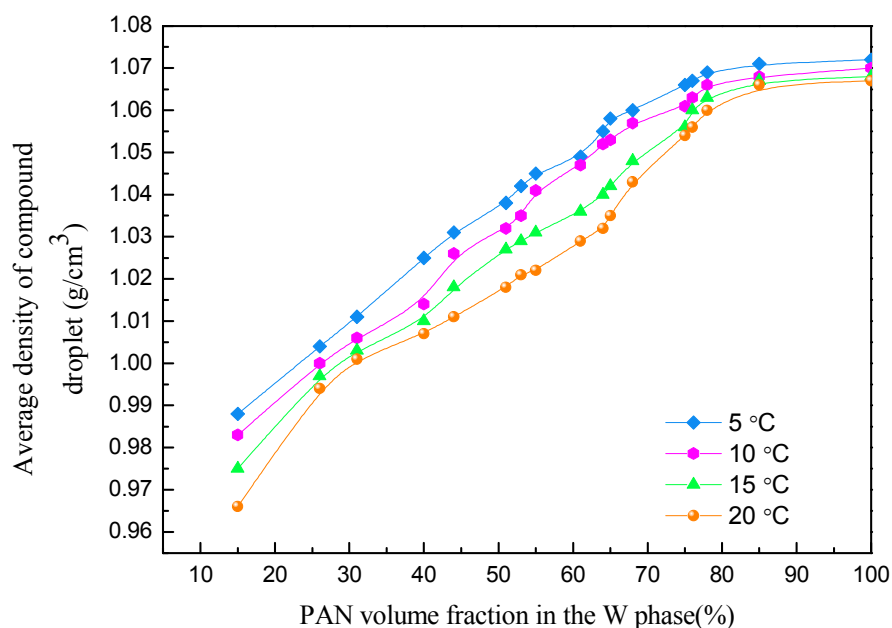


Figure 5. The transformation of the O₁/W compound droplet density at 5 °C, 10 °C, 20 °C, and 30 °C, respectively.

Table 4 Density match level between the O₁/W compound droplet and O₂ phases at different temperature and its effect on OOR and ΔT_w .

Temperature/ (°C)	$\Delta\rho$ ($\Delta\rho=\rho_i-\rho_{O_2}$) / (g/cm ³)	Yields of PAN microspheres with OOR < 2 μm (%)	Yields of PAN microspheres with $\Delta T_w < 9\mu\text{m}$ (%)
5	0.015	84	76
10	0.016	84	74
20	0.025	82	61
30	0.031	71	52

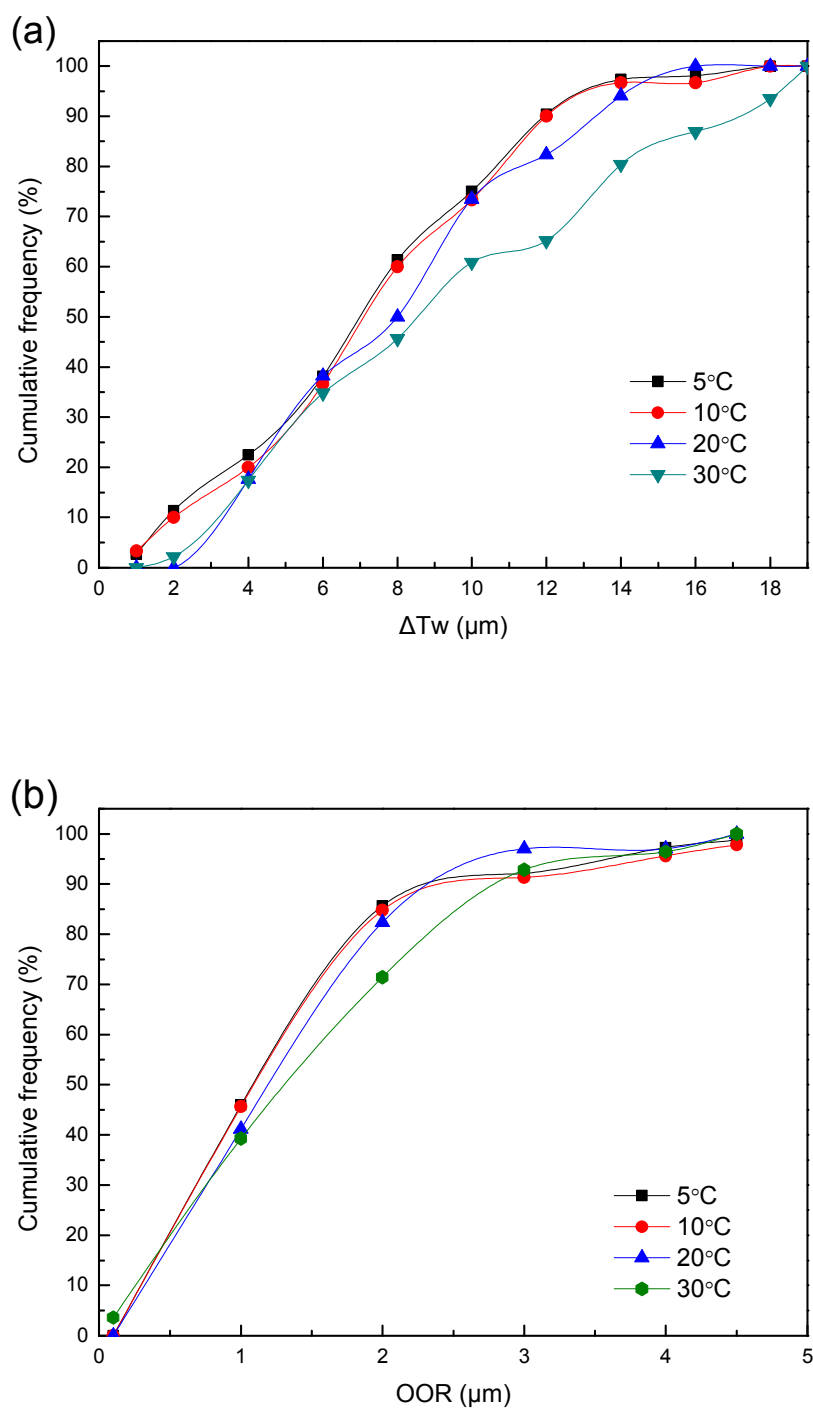


Figure 6. The temperature effects on the quality of PAN microspheres: (a) Wall thickness uniformity. (b) Sphericity.

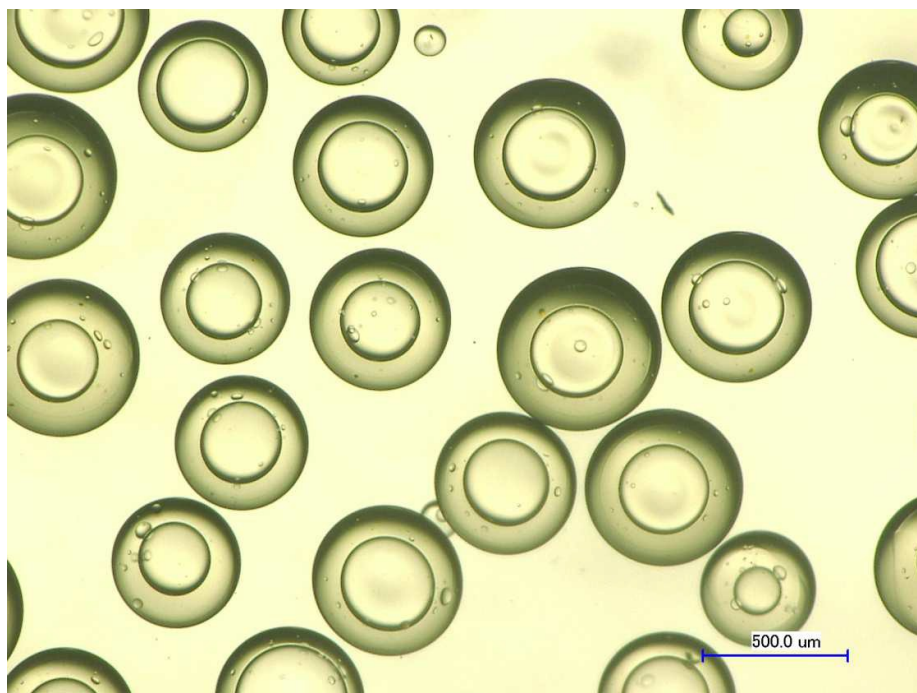


Figure 7. The optical picture of PAN microspheres after solidifying process.

3.3 The influence of viscosity

In the solidification process, the water phase of O_1/W compound droplet contact with the oil phase (O_2), the density gap between the two phases lead to the low density of oil phase floats up, and the high density of O_1/W compound droplet going down.

The layering velocity can be defined as

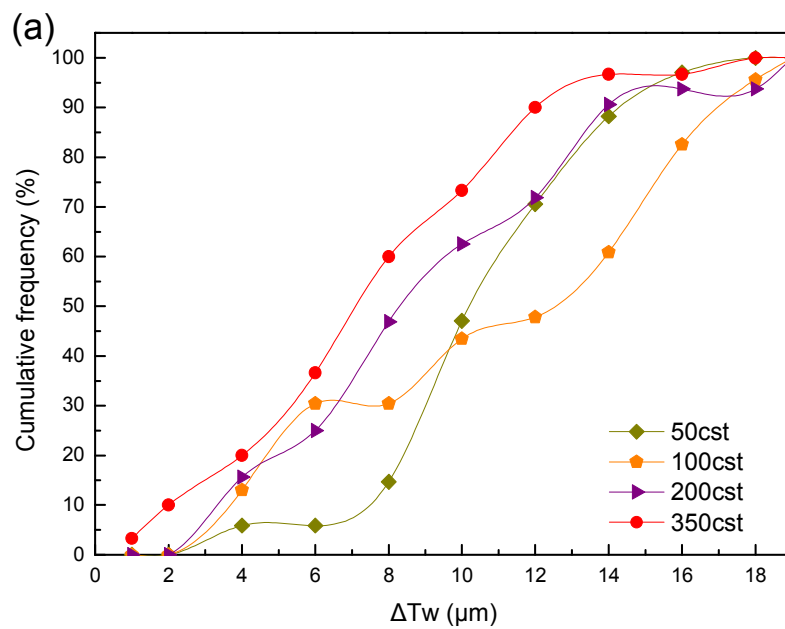
$$V = \frac{2gR(\rho_i - \rho_{o_2})}{9\eta} \quad (15)$$

Here, η is the viscosity of oil phase (O_2). This formation indicated that while the density difference between the O_1/W compound droplet and O_2 phase became smaller or the viscosity of oil phase (O_2) becomes higher, the droplet will be more stable. Additionally, the diffusion coefficient of O_1/W compound droplet would be reduced

following the increase of viscosity of oil phase (O_2), which resulted in the slowdown of the collision frequency of droplets and gathers speed. The deformation of the inner and outer droplets showed great dependency on viscosity and the O_1/W compound droplet displayed larger deformation when the outer phase was more viscous[28,29].

In this experiment, the influences of viscosity on the thickness uniformity of thick-walled PAN microspheres were discussed in the condition of fixed solidifying temperature (10 °C) and the flexible viscosity of the O_2 phase. The corresponding viscosity values of different O_2 phases and W phase are listed in Table 1. The viscosity ratio λ was defined as the ratio between the W phase and the O_2 phase; it was approved that, while the value of λ increased, the percentage of $\Delta T_w < 9 \mu\text{m}$ and $\text{OOR} < 2 \mu\text{m}$ was enhanced (Fig. 8 and Fig.9). In other words, a lower viscosity in the O_2 phase would negatively impact the formation of good wall thickness uniformity and the sphericity of PAN microspheres. However, it is also notable that the influence of viscosity will be limited if its value is overly excessive. For instance, although the 500 cst silicone oil acquired considerable viscosity, the experiment showed that its high viscosity restricted the movement of droplets in the O_2 phase during the solidification process. Similar with the temperature affects, the variation of ΔT_w was more sensitive to the viscosity compared to the OOR, which indicated that the improvement of wall thickness uniformity is more challenging than the enhancement of sphericity. Therefore, in order to ensure that the droplet can be adjusted to perform

good wall thickness uniformity and sphericity, the viscosity ratio λ should be controlled in a certain range.



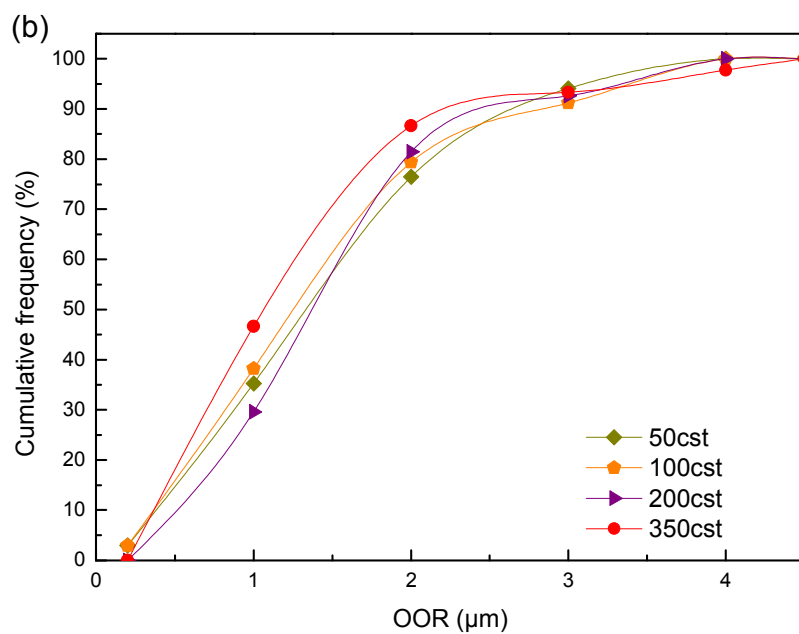


Figure 8. The viscosity influence on the quality of PAN microspheres: (a) Wall thickness uniformity. (b) Sphericity.

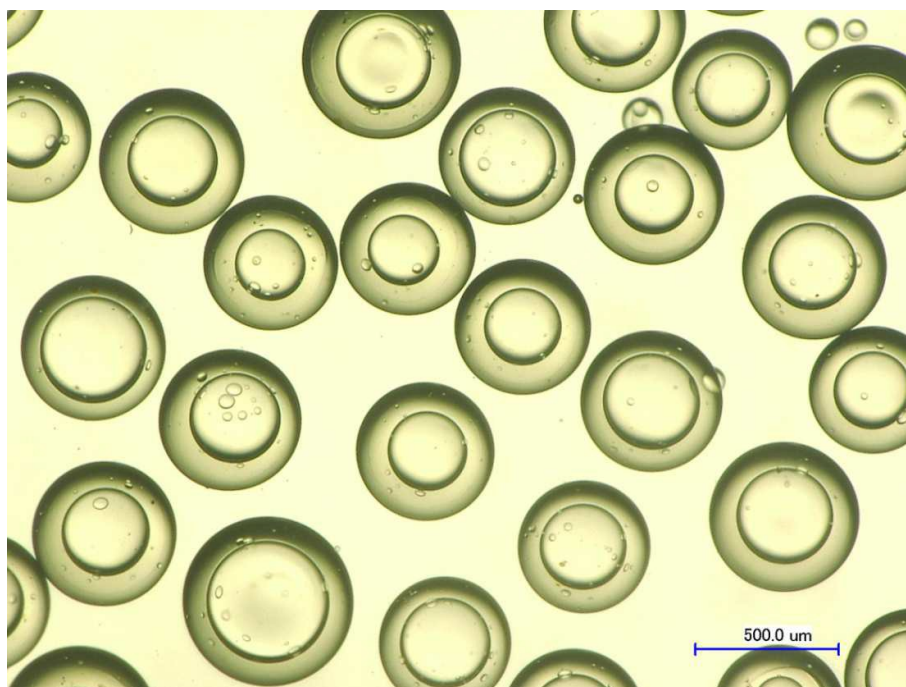


Figure 9. The optical picture of PAN microspheres after solidifying process.

4. Conclusion

In this work, in order to obtain thick-walled PAN microspheres with excellent sphericity and wall thickness uniformity, the temperature effects on the density matching between the O₁/W compound droplet and the O₂ phase, and the influence of viscosity were intensively discussed. When the density of the O₁/W compound droplet was slightly higher than that of the O₂ phase at 10 °C and the viscosity of the O₂ phase was closed to the W phase, high quality PAN microspheres with uniform wall and good sphericity were generated during the solidifying process. Compared to the sphericity, wall thickness uniformity exhibited a higher sensitivity to the solidifying temperature and viscosity of the O₂ phase. The thick-walled PAN microspheres with good wall thickness uniformity were prepared by studying the solidifying temperature and viscosity effects. In the future, how to obtain low density carbon microspheres will be investigated with these good quality PAN microspheres.

5. Acknowledgments

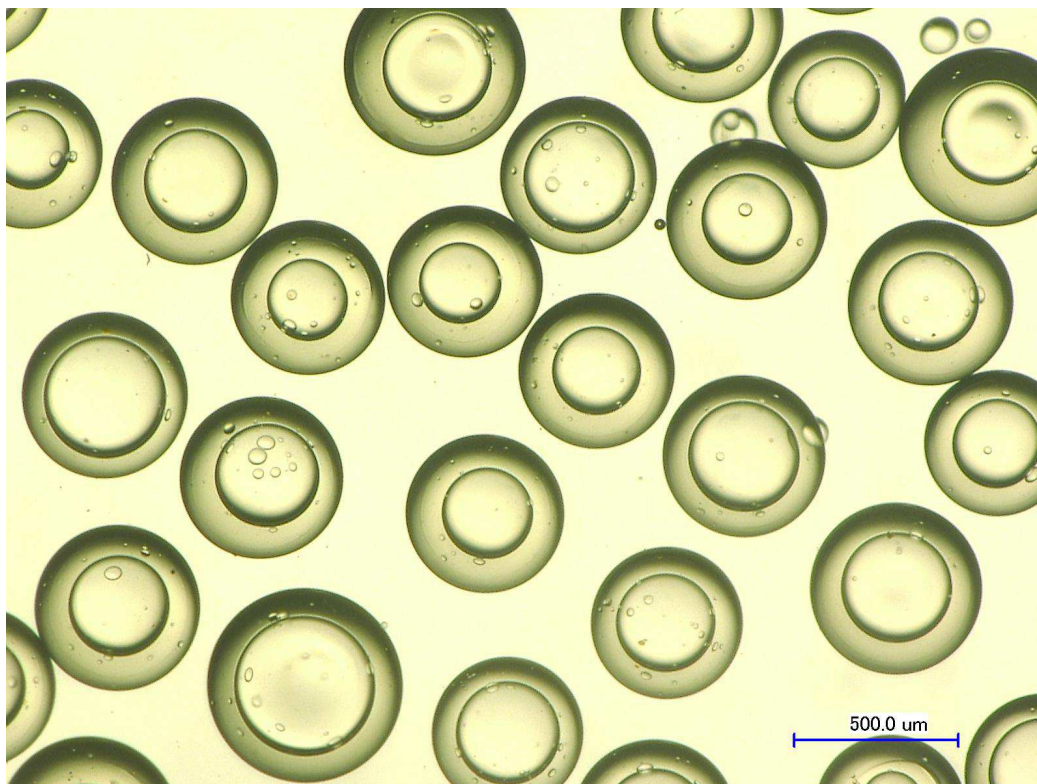
The authors thank for the financial support of pre-research foundation for national science foundation and the China Academy of Engineering Physics Science and Technology Development Fund (2014B0302052).

References

- (1) Kobets, L. P.; Deev, I. S, *Compos Sci Technol*, 1998, 57, 1571-1580.
- (2) Horikawa, T.; Hayashi, J.; Muroyama, K, *Carbon*, 2004, 42, 1625-1633.
- (3) R. Fagaly, L. Brown, R. Stephens, M. Wittman, *Proc. Symp. Fusion Eng.* 10 (1995) 26.

- (4) Peng, H.; Shi Z; Wang W; Chen, S.; Zhang, Z.; Li, B.; Ge, L, *Colloids and Surfaces A: Physicochemical and Engineering Aspects*, 2015, 482, 58-67.
- (5) Ko, T.; Liao, S.; Lin, M. J. *Mater Sci*, 1992, 27, 6071-6078.
- (6) Hou, C.; Qu, R.; Liu, J.; Ying, L.; Wang, C, J. *Appl Polym Sci*, 2006, 100, 3372-3376.
- (7) Sawai, D.; Fujii, Y.; Kanamoto, T, *Polymer*, 2006, 47, 4445-4453.
- (8) An, N.; Xu, Q.; Xu, L. H.; Wu, S. Z. *Advanced Materials Research*, 2006, 11,383-386.
- (9) Liu, J.; Zhang, W. X. *J. Appl Polym Sci*, 2005, 97, 2047-2053.
- (10) Yusof, N.; Ismail, A. F, *J. Anal Appl Pyrol*, 2012, 93, 1-13.
- (11) Bajaj, P.; Roopanwal, A. K, *Journal of Macromolecular Science, Part C: Polymer Reviews*, 1997, 37, 97-147.
- (12) Lattaud, C.; Guillot, L.; Brachais, C. H.; Fleury, E.; Legaie, O.; Couvercelle, J. P, *J. Appl Polym Sci*, 2012, 124, 4882-4888.
- (13) Takagi, M.; Norimatsu, T.; Yamanaka, T.; Nakai, S.; Ito, H, *J. Vac Sci Technol a*, 1991 9, 820-823.
- (14) Takagi, M.; Norimatsu, T.; Yamanaka, T.; Nakai, S, *J. Vac Sci Technol a*, 1991, 9, 2145-2148.
- (15) Nagai, K.; Nakajima, M.; Norimatsu, T.; Izawa, Y.; Yamanaka, T, *Journal of Polymer Science Part A: Polymer Chemistry*, 2000, 38, 3412-3418.
- (16) Schroen Carey, D.; Overturf III, G. E.; Reibold, R.; Buckley, S. R.; Letts, S. A.; Cook, R, *J. Vac Sci Technol a*, 1995, 13, 2564-2568.
- (17) Overturf III, G. E.; Cook, R.; Letts, S. A.; Buckley, S. R.; McClellan, M. R.; Schroen-Carey, D., *Fusion Sci Technol* 1995, 28, 1803-1808.
- (18) Takagi, M.; Cook, R.; Stephens, R.; Gibson, J.; Paguio, S., *Fusion Sci Technol* 2000, 38, 46-49.
- (19) Cook, R. C.; Gresho, P. M.; Hamilton, K. E., *JOURNAL-MOSCOW PHYSICAL SOCIETY* 1998, 8, 221-226.
- (20) Takagi, M.; Cook, R.; Stephens, R.; Gibson, J.; Paguio, S., *Fusion Sci Technol* 2000, 38, 50-53.
- (21) Streit, J.; Schroen, D., *Fusion Sci Technol* 2003, 43, 321-326.
- (22) Paguio, R. R.; Frederick, C. A.; Hund, J. F., *Polymeric Materials: Sci. & Eng* 2006, 95, 872.
- (23) Bei, Z.; Jones, T. B.; Tucker-Schwartz, A, *J. Electrostat*, 2009, 67, 173-177.
- (24) Liu, M.; Chen, S.; Bo Qi, X.; Li, B.; Shi, R.; Liu, Y.; Chen, Y.; Zhang, Z, *Chem Eng J*, 2014, 241,466-476.
- (25) Peng, H.; Xu, Z.; Chen, S.; Zhang, Z.; Li, B.; Ge, L, *Colloids and Surfaces A: Physicochemical and Engineering Aspects*, 2015, 468, 271-279.

- (26) McQuillan, B. W.; Greenwood, A., FUSION TECHNOLOGY-ILLINOIS- 1999, 35, 194-197.
- (27) Mishra, K. K.; Khardekar, R. K.; Singh, R.; Pant, H. C, Pramana, 2002, 59, 113-131.
- (28) Qu, X.; Wang, Y, Physics of Fluids (1994-present), 2012, 24,123302.
- (29) Delaby, I.; Ernst, B.; Germain, Y.; Muller, R, Journal of Rheology (1978-present), 1994, 38:1705-1720.



Thick-walled PAN microspheres with good wall thickness uniformity and sphericity were obtained by adjusting the solidifying temperature and the viscosity of O_2 phase.